Deposition of Thermally Unstable Molecules with the Spray-Jet Technique on Au(111) Surface

Hitoshi Suzuki,* Toshiki Yamada, Toshiya Kamikado, Yoshishige Okuno, and Shinro Mashiko

Kansai Advanced Research Center, National Institute of Information and Communications Technology, 588-2 Iwaoka, Nishi-ku, Kobe 651-2492, Japan

Received: March 16, 2005; In Final Form: May 17, 2005

A porphyrin derivative (5,15-bis(4-ethynylphenyl)-10,20-bis(3,5-di-*tert*-butylphenyl)porphyrin: *trans*-BETBPP) possessing chemically reactive substituents was successfully deposited on an Au(111) surface with a new molecular beam deposition system with use of a spray-jet technique (Spray-jet-MBD) without denaturing the molecules. The deposited molecular overlayers were observed at 77 K under ultrahigh vacuum condition by scanning tunneling microscopy (STM). They form two different overlayer structures: a linear arrangement and a square lattice structure. In these overlayers, some molecules were accidentally moved by STM tip agitation, which indicates that the molecules were not polymerized during the deposition process.

1. Introduction

Organic molecules deposited by thermal evaporation on metal substrates have been extensively studied with great interest because of their superstructures that reflect their intrinsic intermolecular interactions. Scanning tunneling microscopy (STM), operated in ultrahigh vacuum (UHV), has become one of the most powerful and indispensable tools for observing these molecular superstructures and it has elucidated the molecular internal structures of large organic molecules and their overlayer structures deposited on a substrate.[1−8] The electronic properties of molecules were also characterized at subnanometer resolutions.[9,10] However, the successful results from the UHV STM observations of the molecules on metal surfaces were obtained for molecules that were deposited by thermal evaporation. Small organic molecules that can be easily evaporated from crucibles with proper heating can be deposited on substrates, without risk of contamination, to observe the molecular images with the substrate structures. On the other hand, large molecules, including some oligomers and polymers, are difficult to evaporate by heating because they have a strong van der Waals interaction between the molecules and their long substituents, which are entangled with each other. Thermally unstable molecules, i.e., molecules having reactive substituents, were also especially difficult to evaporate, because these substituents were denatured or polymerized by the heating conducted before the evaporation process. Therefore, STM has not produced enough significant results on these molecules. To observe the molecular overlayer structures and their behaviors for the large or unstable molecules, we have to use a new deposition method that is different from thermal evaporation.

Recently, some research groups have attempted to deposit large molecules, including DNA, polymers, and carbon nanotubes, on metals and/or semiconductor substrates.[11−16] In these studies, the macromolecules dissolved in an organic solvent were directly injected into a vacuum chamber by a microsyringe or pulse valve and were successfully observed with UHV STM. The pressure during the deposition was typically 1.3×10^{-1} Pa because it did not have a differential pumping system.[11] They did not confirm directly whether the molecules were separated from each other during the injection process.

The spray-jet technique is another promising way to deposit nonvolatile molecules onto a clean substrate surface, because it can produce a high-quality molecular beam of neutral nonvolatile molecules under high vacuum condition (1.3×10^{-3} Pa). In this method, the solution, including the target molecule, was made into a mist with an ultrasonic nebulizer and is introduced into the vacuum chamber through a pulse valve and skimmers. A molecular beam of nonvolatile molecules was produced in the main chamber, while the solvent was reduced during passing through some chambers that were differentially pumped. Using a combination of this technique and multiphoton ionization time-of-flight mass spectroscopy (MPI-TOFMS), we have succeeded in obtaining a mass spectrum of single target molecules, such as dendrimers, dye molecules, and porphyrin derivatives.[17−19] We have applied the spray-jet technique to the deposition of a small molecule on a clean Au(111) surface; a subphthalocyanine derivative was successfully deposited on the surface and the molecular structure observed with UHV STM is comparable to that prepared by thermal evaporation.[20] However, we have not investigated the performance of the spray-jet technique for deposition of nonvolatile molecules because the subphthalocyanine derivative can be evaporated for deposition by the usual thermal evaporation.[7,21]

Here, we chose a thermally unstable molecule, a porphyrin derivative, to study the performance of the molecular beam deposition system using the spray-jet technique (Spray-jet-MBD). The molecule had two ethynyl groups that were reactive substituents. The deposited overlayer structure was observed by UHV STM at 77 K and examined with theoretically calculated models.

2. Experimental Section

2.1. Molecule. The molecule used in this study is 5,15-bis-(4-ethynylphenyl)-10,20-bis(3,5-di-*tert*-butylphenyl)porphyrin (*trans*-BETBPP) (Figure 1). This molecule is a derivative of tetrakis(di-*tert*-butylphenyl)porphyrin (TBPP) that is popularly examined in SPM measurements.[1,22−26] TBPP has four di-*tert*-

* Corresponding author. E-mail:suzuki@nict.go.jp. Phone: +81-78-969-2253. Fax: +81-78-969-2259.

10.1021/jp051388t CCC: $30.25
Published on Web 06/18/2005

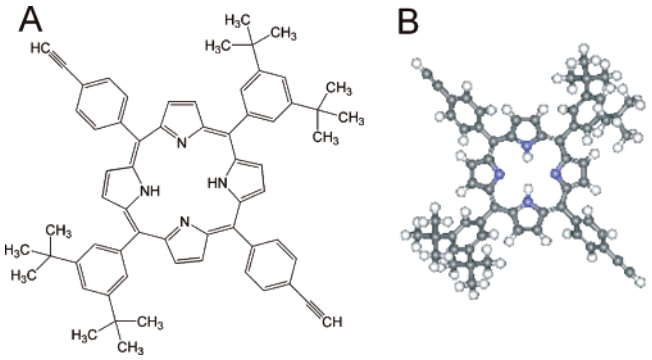

Figure 1. Molecular structure of *trans*-BETBPP.

butylphenyl groups bound to the central porphyrin ring. In previous studies on this molecule, a bulky substituent, the di-*tert*-butylphenyl group, appeared as one or two bright protrusions depending on the relative position of the two butyl groups and on the sharpness of the STM probe, i.e., some STM images of TBPP have eight protrusions with the central porphyrin ring[22,23] and some showed four.[1,24] It represents that the contrast of the image reflects the morphological structure as well as the electronic structure. The *trans*-BETBPP molecule used in this study has two di-*tert*-butylphenyl groups in the trans position of the porphyrin ring and two ethynylphenyl groups. The ethynyl groups are triple bonds having reactivity, which have been reported to show polymerization with each other by the application of high current under a STM probe.[27] This reactive substituent prevents thermal evaporation of the molecule. In previous experiments, *trans*-BETBPP molecules were not evaporated by heating even at 570 K while a similar porphyrin with a single ethynyl group was evaporable with proper heating.[28] The denaturalization of the molecules is likely to occur in the range from 420 to 570 K. The *trans*-BETBPP molecule was dissolved in chloroform (0.3 mM) for the deposition by the spray-jet technique.

2.2. Deposition System and STM. The details for the Spray-jet-MBD system and the experimental procedure are explained elsewhere.[20] The solution, which includes the *trans*-BETBPP molecule, was made into a mist with an ultrasonic nebulizer and introduced into the vacuum chambers through a pulse valve. The chambers consisted of four parts differentially pumped that were separated by skimmers and gate valves. The base pressure of the final stage chamber was approximately 5×10^{-8} Pa. The pressure rose to approximately the 10^{-4} Pa range during the deposition and it recovered to the 10^{-7} Pa range in 30 min after the deposition.

The molecule was deposited at room temperature on an Au(111) surface previously prepared on freshly cleaved mica. The Au(111) surface was cleaned by repeated cycles of Ar-ion sputtering (1 kV) and successive annealing at 800 K. After deposition, the sample was transferred to the preparation chamber of a UHV STM system (LTSTM, Omicron) with a transfer chamber, to keep the sample in the vacuum condition. Then, it was heated to approximately 400 K to remove any solvent remaining on the surface. The sample was cooled to 77 K in the STM stage. The STM measurement was carried out at 77 K under the UHV condition ($<10^{-8}$ Pa) with a chemically etched W probe. The bias voltage was approximately -2 V and the tunneling current was around 20 pA, which were similar to our previous studies on the STM observations of organic molecules.[7,21]

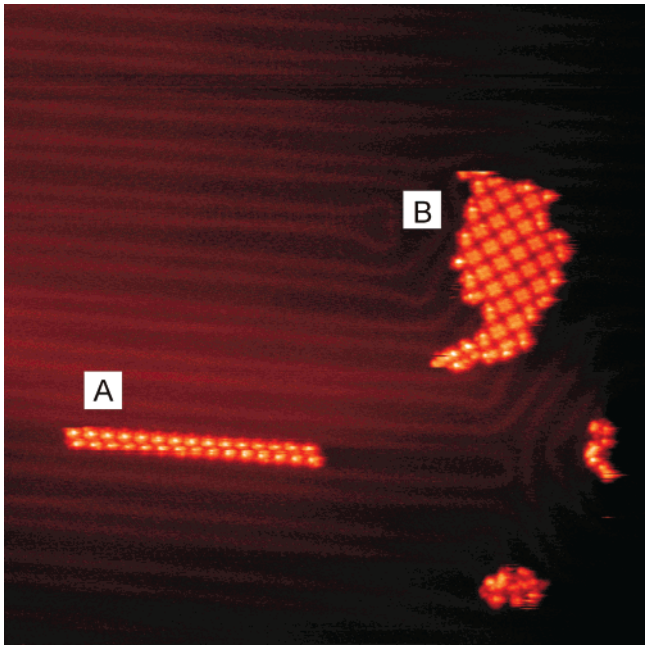

Figure 2. STM image of *trans*-BETBPP overlayer on Au(111) surface prepared by the spray-jet technique (image size = 80 × 80 nm^2, $V = -2.051$ V, $I = 22$ pA).

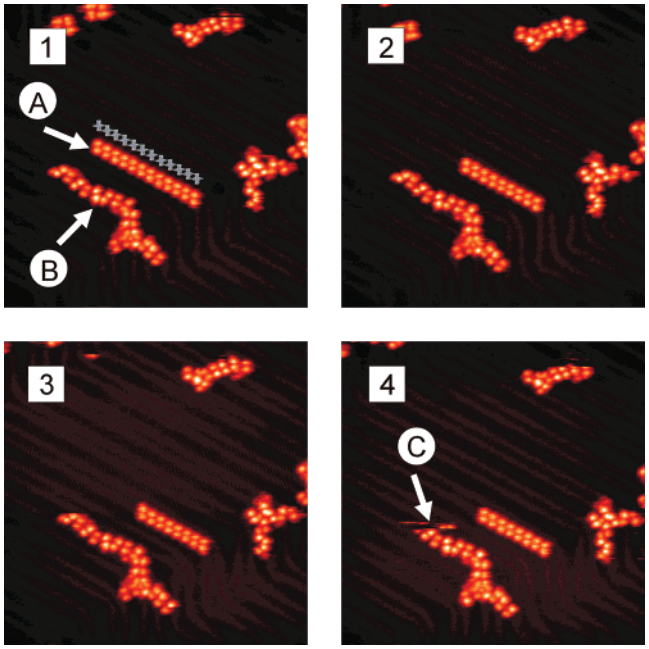

Figure 3. Time series of the linear arrangements of *trans*-BETBPP (image size = 60 × 60 nm^2, $V = -1.853$ V, $I = 24$ pA).

3. Results and Discussion

An STM image of the *trans*-BETBPP overlayer on an Au(111) surface is shown in Figure 2. The image was obtained from an area where the adsorbed density of the molecule is low. The *trans*-BETBPP molecules form two different overlayer structures in Figure 2. One is a linear arrangement (Figure 2A) and the other is a square lattice (Figure 2B). In some STM images, a linear/amorphous arrangement is also observed (Figure 3-4B). In the linear arrangement, the bulky substituents, which are *tert*-butyl groups, appear as bright spots, which is the same as those in previous reports on TBPP molecules.[1,23] A single *trans*-BETBPP molecule is identified by a pair of bright spots

in this figure, because it has only two di-*tert*-butylphenyl groups, and this line consists of the 15 molecules. In this experiment, it was difficult to distinguish a single *tert*-butyl group from the other one bound to the same phenyl group because of the dullness of the STM probe. A single isolated molecule is not observed because the heating process is likely to agitate the molecular diffusion to form the stable structures.

This linear arrangement is similar to the wire-like structure of the cyano-TBPP overlayer on an Au(111) surface.[29] However, we have obtained an STM image of the curved *trans*-BETBPP linear structure in which the molecule forms a varied angle with the neigboring one (Figures 3-1B), which is different from the configuration of the cyano-TBPP line. In the case of the cyano-TBPP, the molecules formed a wire-like structure in which the cyano group made a hydrogen bond with one next to it because of the strong polarity in the cyano group. On the other hand, the ethynyl group does not have a strong polarity; therefore, they do not form hydrogen bonds with each other. In addition, most of the *trans*-BETBPP molecules align along the stripe of the herringbone structure, which is different from that of the cyano-TBPP bridge over the elbow regions of the herringbone structure. This difference suggests that the linear structure formed by the *trans*-BETBPP molecules is mainly dominated by the substrate morphology. The herringbone reconstructed surface of Au(111) has low ridges of boundaries of hcp phase and fcc phase.[34] This surface morphology increases the stability of the adsorbates, including the *trans*-BETBPP.

The linear arrangement is not a stable structure because the ethynyl group does not have the polarity to form a bond, like the hydrogen bond. Figure 3 (panels 1−4) shows a series of STM images of the alignment of the *trans*-BETBPP molecules successively obtained. In the first image (Figures 3-1), 12 molecules form the linear arrangement (A). The next image (Figures 3-2) has only 9 molecules. We think that the three missing molecules were removed by the scanning STM probe. This molecular number reduction continues in the third image (Figure 3-3); the number becomes 8. In the fourth image (Figures 3-4), there are still 8 molecules in the line but some streaks representing the motion of the molecules appear at the top of a linear/amorphous arrangement (C), which indicates that two molecules are moved during the scanning. This indicates that the molecules are separated from each other, so the scanning probe can easily displace them. It also shows that the spray-jet technique can deposit them without polymerization. The molecules in the linear/amorphous arrangement show almost the same stability as the linear arrangement because their ethynyl groups are also close to the neighboring one.

The square lattice structure is also frequently observed along with the linear structure in the *trans*-BETBPP overlayers. Figure 4 is a magnified STM image of the square lattice. The overlaid molecular models represent a plausible model of the structure and the two white arrows indicate the unit vectors of the lattice. In our model, this overlayer structure consists of two basis and two lattice vectors forming about an 89.2° angle ($\sqrt{73} \times 2\sqrt{19}$). The difference in the length of the vectors is 2% and the angle is nearly 90°, which is very close to a square lattice. It agrees very well with the observed molecular overlayer. A white outline with two circles represents a single *trans*-BETBPP molecule. In this STM image, *tert*-butyl groups show up in a bright contrast but they are difficult to distinguish from those of the neighboring molecules. A pair of weak bright spots indicated by the small white circles in the outline represent an inner structure of the porphyrin ring, which has been previously reported.[23]

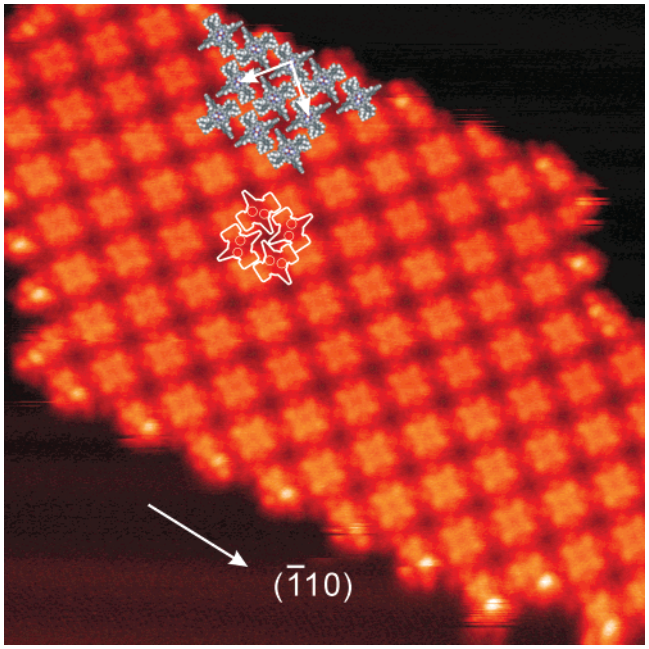

Figure 4. STM image of *trans*-BETBPP overlayer forming square lattice (image size = 30 × 30 nm^2, $V = -2.051$ V, $I = 22$ pA).

To confirm the effect of the intermolecular interaction between the ethynyl groups, we did quantum chemical calculations on ethynylbenzene, its dimer, and its tetramer to determine their stable structures, aggregated through the interaction between the ethynylphenyl groups, which is a partial model of a *trans*-BETBPP. Ethynylbenzene was used as a simplified model for the ethynylphenyl group of *trans*-BETBPP because porphyrin with an ethynylphenyl group and other substituents were too large to calculate their structures. The calculations were carried out with the 6-31G* basis set[30] at the B3LYP level of theory,[31] using the Gaussian03 program package.[32] For the optimization of the tetramer, we used a fast optimization method recently developed in our group[33] to reduce the computational time. Also note that for all the calculations we used ultrafine integration grid3 (99 radial shells and 590 angular points) for numerical integration. We had to use this integration because we were unable to completely optimize the tetramer structure when using a normal grid3 (75 radial shells and 302 angular points), because a smaller number of grids would have resulted in a larger number of errors in the numerical integration in density functional calculations.

Figure 5 shows the stable structure of the ethynylbenzene's monomer, dimer, and tetramer and their potential energy and Table 1 shows the differences in the molecular interaction energies. The difference in molecular interaction energies between the monomer and the dimer is −1.60 kcal/mol, which shows that the dimer configuration is more stable than the two independent monomers. The difference in the energy between the benzonitrile monomer that is a part of cyano-TBPP and its dimer is −5.33 kcal/mol.[35] Comparing these energies, the intermolecular interaction of the *trans*-BETBPP is weaker than the cyano-TBPP, so the linear structure of the *trans*-BETBPP is more unstable than the cyano-TBPP. The stable dimer structure is a diagonally crossed configuration. This diagonal configuration does not match the structure actually observed because this calculation does not include the influence of the substrate. However, the tendency of the ethynyl group to attract the other benzene ring must reflect the actual structure, a linear arrangement. In addition, the interaction energy of the dimers, calculated under the forced conditions that the molecules exist

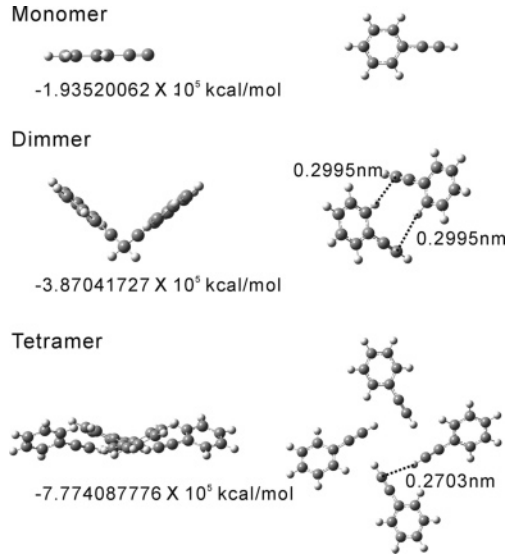

Figure 5. Optimized stable structures of ethynylbenzene monomer, dimer, and tetramer, and distances and potential energies. The structure on the right of each labeled figure is the structure viewed from the top of the left figure. The energy of the intermolecular interaction in the dimer is 1.60 kcal/mol and that in the tetramer is 7.52 kcal/mol.

TABLE 1: Difference between Calculated Interaction Energies for Ethynylbenzene and Benzonitrile Clusters.

	ΔE (kcal/mol)
ethynylbenzene$_{\text{dimer}-2\times\text{monomer}}$	−1.60
ethynylbenzene$_{\text{tetramer}-2\times\text{dimer}}$	−4.32
benzonitrile$_{\text{dimer}-2\times\text{monomer}}$	−5.33 (ref 35)

in the same plane, is −1.08 kcal/mol. It is almost the same as that of the diagonally crossed structure.

Four ethynylbenzenes form a tetramer configuration, where the hydrogen from the ethynylbenzene group faces to the side of the neighboring ethynyl groups. The difference in energies between the dimer and tetramer is −4.32 kcal/mol. This shows that the tetramer configuration has a stabler energy than the dimer configuration. This result agrees with the fact that a square lattice structure is more stable than a linear arrangement during our STM measurements. The tetramer configuration agrees well with the plausible model obtained from the STM image. In the model, the distance between the hydrogen atom of the ethynylbenzene and the carbon atom of the neighboring ethynylbenzene is 0.27 nm. The actual distance between the hydrogen atom and the carbon atom is estimated to be 0.3 to 0.4 nm from the obtained STM image.

Considering the results in the theoretical calculation, we suppose that the square lattice should increase rather than the linear structure by annealing. However, in the experiments, we did not observe obvious dependence of the existence ratio of the linear structure to the square lattice structure on surface coverage, annealing temperature (<420 K), or annealing time. We think that the influence of the substrate, which is not included in the calculation, might be another factor to increase the linear and the linear/amorphous structures.

4. Conclusion

trans-BETBPP molecules were successfully deposited on an Au surface with the Spray-jet-MBD system and their overlayer structures were clearly observed with a UHV STM. The obtained STM images have a comparable quality to previous STM images of organic molecules that were deposited by thermal evaporation. They elucidated that *trans*-BETBPP molecules formed different overlayer structures depending on the substrate's morphology and intermolecular interaction. The results showed that the Spray-jet-MBD system is useful in depositing unstable molecules having reactive substituents. We believe that this method can be applied to the deposition of other nonvolatile molecules, including oligomers, polymers, proteins, and other biological molecules, to improve the quality of the target molecules to be characterized.

References and Notes

(1) Jung, T. A.; Schlittler, R. R.; Gimzewski, J. K. *Nature* **1997**, *386*, 696.
(2) Scudiero, L.; Barlow, D. E.; Hipps, K. W. *J. Phys. Chem. B* **2000**, *104*, 11899.
(3) Scunack, M.; Petersen, L.; Kühnle, A.; Lægsgaard, E.; Stensgaard, I.; Johannsen, I.; Basenbacker, F. *Phys. Rev. Lett.* **2001**, *86*, 456.
(4) Wild, M.; Berner, S.; Suzuki, H.; Yanagi, H.; Schlettwein, D.; Ivan, S.; Baratoff, A.; Guentherodt, H.-J.; Jung, T. A. *ChemPhysChem* **2002**, *3*, 881−885.
(5) Kühnle, A.; Linderoth, T. R.; Hammer, B.; Besenbacher, F. *Nature* **2002**, *415*, 891−893.
(6) Barth, J. V.; Weckesser, J.; Trimarchi, G.; Vladimirova, M.; Vita, A. D.; Cai, C.; Brune, H.; Günter, P.; Kern, K. *J. Am. Chem. Soc.* **2002**, *124*, 7991.
(7) Suzuki, H.; Miki, H.; Yokoyama, S.; Mashiko, S. *Thin Solid Films* **2003**, *438*−*439*, 97−100.
(8) Theobald, J. A.; Oxtoby, N. S.; Phillips, M. A.; Champness, N. R.; Beton, P. H. *Nature* **2003**, *424*, 1029−1031.
(9) Langlais, V. J.; Schlittler, R. R.; Tang, H.; Gourdon, A.; Joachim, C.; Gimzewski, J. K. *Phys. Rev. Lett.* **1999**, *83*, 2809.
(10) Nazin, G. V.; Qiu, X. H.; Ho, W. *Science* **2003**, *302*, 77−81.
(11) Tanaka, H.; Hamai, C.; Kanno, T.; Kawai, T. *Surf. Sci. Lett.* **1999**, *432*, L611.
(12) Tanaka, H.; Kawai, T. *J. Vac. Sci. Technol. B* **1997**, *15*, 602.
(13) Kasai, H.; Tanaka, H.; Okada, S.; Oikawa, H.; Kawai, T.; Nakanishi, H. *Chem. Lett.* **2002**, 696.
(14) Kim, Y.; Komeda, T.; Kawai, M. *Phys. Rev. Lett.* **2002**, *89*, 126104.
(15) Terada, Y.; Choi, B.-K.; Heike, S.; Fujimori, M.; Hashizume, T. *J. Appl. Phys.* **2003**, *93*, 10014.
(16) Terada, Y.; Choi, B.-K.; Heike, S.; Fujimori, M.; Hashizume, T. *Jpn. J. Appl. Phys.* **2003**, *42*, 4739.
(17) Yamada, T.; Ge, M.; Shinohara, H.; Kimura, K.; Mashiko, S. *Chem. Phys. Lett.* **2003**, *379*, 458.
(18) Yamada, T.; Shinohara, H.; Ge, M.; Kimura, K.; Mashiko, S. *Thin Solid Films* **2003**, *438*−*439*, 7.
(19) Yamada, T.; Shinohara, H.; Ge, M.; Mashiko, S.; Kimura, K. *Chem. Phys. Lett.* **2003**, *370*, 132.
(20) Yamada, T.; Suzuki, H.; Miki, H.; Mashiko, S. *J. Phys. Chem. B* **2005**, *109*, 3183.
(21) Suzuki, H.; Miki, H.; Yokoyama, S.; Mashiko, S. *J. Phys. Chem. B* **2003**, *107*, 3659.
(22) Moresco, F.; Meyer, G.; Rieder, K.-H.; Tang, H.; Gourdon, A.; Joachim, C. *Phys. Rev. Lett.* **2001**, *86*, 672.
(23) Yokoyama, T.; Yokoyama, S.; Kamikado, T.; Mashiko, S. *J. Chem. Phys.* **2001**, *115*, 3814.
(24) Loppacher, Ch.; Guggisberg, M.; Pfeiffer, O.; Meyer, E.; Bammerlin, M.; Lüthi, R.; Schlittler, R.; Gimzewski, J. K.; Tang, H.; Joachim, C. *Phys. Rev. Lett.* **2003**, *90*, 066107.
(25) Tanaka, S.; Suzuki, H.; Kamikado, T.; Mashiko, S. *Thin Solid Films* **2003**, *438*−*439*, 56−60.
(26) Tanaka, S.; Suzuki, H.; Kamikado, T.; Mashiko, S. *Nanotechnology* **2004**, *15*, S87−S90.
(27) Okawa, Y.; Aono, M. *Nature* **2001**, *409*, 683.
(28) Sekiguchi, T. Personal communication.
(29) Yokoyama, T.; Yokoyama, S.; Kamikado, T.; Okuno, Y.; Mashiko, S. *Nature* **2001**, *413*, 619.
(30) Binkley, J. S.; Pople, J. A.; Hehre, W. J. *J. Am. Chem. Soc.* **1980**, *102*, 939.
(31) Becke, A. D. *J. Chem. Phys.* **1993**, *98*, 5648.
(32) Frisch, M. J.; Trucks, G. W.; Schlegel, H. B.; Scuseria, G. E.; Robb, M. A.; Cheeseman, J. R.; Montgomery, J. A., Jr.; Vreven, T.; Kudin, K. N.; Burant, J. C.; Millam, J. M.; Iyengar, S. S.; Tomasi, J.; Barone, V.; Mennucci, B.; Cossi, M.; Scalmani, G.; Rega, N.; Petersson, G. A.; Nakatsuji, H.; Hada, M.; Ehara, M.; Toyota, K.; Fukuda, R.; Hasegawa, J.; Ishida, M.; Nakajima, T.; Honda, Y.; Kitao, O.; Nakai, H.; Klene, M.; Li, X.; Knox, J. E.; Hratchian, H. P.; Cross, J. B.; Adamo, C.; Jaramillo, J.; Gomperts, R.; Stratmann, R. E.; Yazyev, O.; Austin, A. J.; Cammi, R.;

Pomelli, C.; Ochterski, J. W.; Ayala, P. Y.; Morokuma, K.; Voth, G. A.; Salvador, P.; Dannenberg, J. J.; Zakrzewski, V. G.; Dapprich, S.; Daniels, A. D.; Strain, M. C.; Farkas, O.; Malick, D. K.; Rabuck, A. D.; Raghavachari, K.; Foresman, J. B.; Ortiz, J. V.; Cui, Q.; Baboul, A. G.; Clifford, S.; Cioslowski, J.; Stefanov, B. B.; Liu, G.; Liashenko, A.; Piskorz, P.; Komaromi, I.; Martin, R. L.; Fox, D. J.; Keith, T.; Al-Laham, M. A.; Peng, C. Y.; Nanayakkara, A.; Challacombe, M.; Gill, P. M. W.; Johnson, B.; Chen, W.; Wong, M. W.; Gonzalez, C.; Pople, J. A. *Gaussian 03*, Revision B.05; Gaussian, Inc.: Pittsburgh, PA, 2003.

(33) Okuno, Y.; Mashiko, S. *Chem. Phys. Lett.* **2004**, *401*, 35−39.

(34) Wöll, Ch.; Chiang, S.; Wilson, R. J.; Lippel, P. H. *Phys. Rev. B* **1989**, *39*, 7988.

(35) Okuno, Y.; Yokoyama, T.; Yokoyama, S.; Kamikado, T.; Mashiko, S. *J. Am. Chem. Soc.* **2002**, *124*, 7218.